한국측지학회지, 第6卷, 第1號, pp. 13~24, 1988年 6月 30日

Multiple-Method에 依한 圓形構造物 變形測定의 正確度 向上에 關한 硏究

A Study on the Improvement of Accuracy for Deformation Measurement of Circular Structures by Multiple Method

Raymond J. Hintz*
姜 準 默**
Kang Joon—Mook
吳 元 鎭***
Oh Won—Jin

要 旨

圓形 構造物의 表面에 對한 三次元 位置 決定은 여러 面에서 그 應用이 期待된다. 構造物의 診斷을 考慮해 볼때 이것은 광범위한 범주에서 하나의 의미있는 Topic이 될 것이며, 이러한 位置 決定을 함에 있어 수렴寫眞의 活用은 從來의 測量에 비해 많은 利點을 가지고 있다. 本 論文은 Metric과 Non-metric Camera를 利用하여 圓筒形의 被寫體를 수렴寫眞으로 촬영하고 Bundle-Adjustment에 의해 그 結果를 考察한 것이다. Bundle-Adjustment에 의한 誤差 解析으로부터 標準 誤差를 比較함과 아울러 Metric과 Non-metric Camera로부터 얻은 被寫體의 三次元 座標도 比較하였다.

Abstract

The determination of three-dimensional positions on a circular or cylindrical surface covers a variety of applications. As an example, consider the monitoring of structures, which is an important topic in the broad category of deformation analysis. The use of convergent photography in determination of these positions has the many advantages over survey based procedures. This paper illustrates results from bundle adjustments derived from convergent photography of a cylindrical object, with both metric and non-metric cameras utilized in the test. In addition to standard error comparisons resulting from the error analysis provided by the bundle adjustments, object space coordinates resulting from metric and non-metric camera network geometries will also be compared.

1. Introduction

The use of convergent photographs of targeted object points has been utilized, in a wide variety of applications, for determination of precise relative three-dimensional positions. For a recent discussion of applications, one can refer to the collection of articles in *Close-Range Photogrammetry and Surveying: State-of-the-Art* (numerous authors, 1985). Brown (1980)[2] has shown the convergent approach can result in a more even error distribution for the coordinates of the object points. This is in comparison to the traditional stereo approach, which will inevitably result in larger error estimates in the coordinates whose axis parallels the camera axes.

* University of Maine
** 忠南大學校 工科大學 副敎授
*** 忠南大學校 大學院 博士課程

Situations exist, such as the measurement of points on a cylindrical or spherical object, where it is impossible to collect all object point information in a single stereo pair. Collection of information with several stereo pairs, followed by merging of the data to a common coordinate system via coordinate transformations, could be accomplished, but it is apparent a simultaneous solution for all object point coordinates is desired.

The obvious solution to the problem is a non-topographic approach which involves measurement of the targeted object points a monoscopic mode of data collection, followed by a bundle adjustment (see Brown, 1980, or Wolf, 1983, for a complete discussion of this approach[2)6)] of the collected information. This provides the statisticall, best solution for the given measurements.

The measurement, by convergent photography, of a cylindrical structure 90cm. tall and 70cm. in horizontal diameter, is described in detail. Three circular rows of 12 photos each, with the top and bottom rows positioned so that their respective inclination and declination angles are each 15 degrees, were exposed with a Wild P-31 metric camera (principal distance of 105.04 mm.) at an object distance of approximately 1.8meters. The middle row was duplicated with 12 photos exposed from the same positions with a non-metric Yashica MAT-124 70mm. format camera(principal distance of 80.00 mm). The non-metric photos were also reduced by bundle adjustment procedures utilizing the image format corners in delineation of a photocoordinate system (Hintz, 1985).[5)]

The standard errors resulting from the different camera geometries and control point configurations will be illustrated, along with a comparison of coordinate differences between the metric and non-metric results. All photohraphic measurements were performed in a monoscopic mode using a Kern DSR-1 analytical streoplotter, so it should be noted that the same results could have been obtained using a monocomparator of similar coordinate measurement resolution. All adjustments were performed on an IBM-AT microcomputer.

The resuits presented here hopefully represent a practical discussion of obtainable accuracies given a standard cylindrical problem, and provide readers with a "how to" approach to the problem.

2. Experimental Investigation

(1) Generation of Approximations for Exposure Station and Object Space Unknowns

Due to linearization of the collinearity equations in the bundle adjustment solution, approximations are required for all unknowns. This involves three coordinate approximations (X_A, Y_A, Z_A) for each object point, and six approximations for each camera exposure station. The exposure station unknowns are represented by three coordinates (X_L, Y_L, Z_L) plus three rotation angles (omega, phi, kappa) which represent the angular relation of the X, Y, Z camera axes to the same object space coordinate axes respectively.

One reason measurement techniques, which use least squares analysis, have been misunderstood is the requiring of approximations for unknowns when the observation equations require linearization. Brown (1980)[2)] has demonstrated ,how computerized pre-analysis can overcome most approximation difficulties, but one must also consider that certain potential users of non-topographic photogrammetry may not have access to such a level of au-

tomation. While it is acknowledged that determination of coordinate approximations can be a difficult problem in some adjustment problems, close-range photogrammetry does not usually fall into this group.

Initial coordinate estimates require the delineation of the coordinate origin and the coordinate axes. In the examples illustrated in this paper, the object space X and Y coordinate axes were approximated to be parallel with the photo x and y axes of the first photo (see figure 1), making the object space Z coordinate axis positive towards the first exposure station. There is no reason why post-adjustment coordinates cannot be rotated and translated into any desired coordinate system via three-dimensional coordinate transformations (Wolf, 1983).[6]

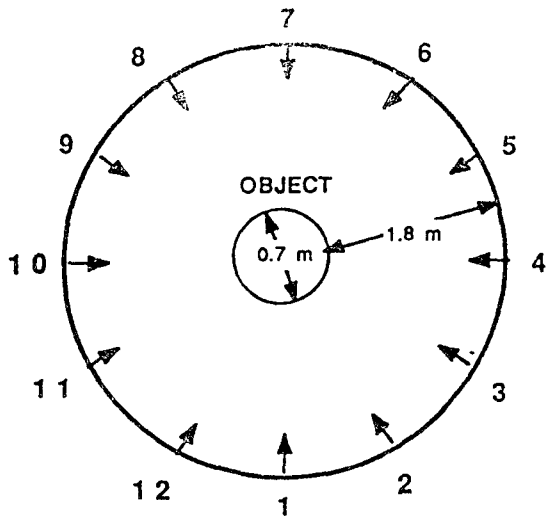

Fig. 1 Relation of camera exposure stations to cylindrical object.

A simple sketch will provide one with sufficient ability to generate coordinate estimates for all object points and camera exposure stations. For the object being studied, estimates within 2 meters of their adjusted values proved sufficient for solution convergence. It is important that the photogrammetrist knows the orientation of his/her object space coordinate axes, which are based strictly on coordinates of the control points in the object space.

The confusion in initial approximation generation in non-topographic photogrammery usually centers on estimating the angular unknowns of the exposure stations. This is because the angular approximations build upon any previous rotations, i.e., the second rotation angle is based on the coordinate axes after the first rotation. The third rotation angle is based on a twice rotated coordinate system.

The collinearity equations used in developing the bundle adjustment software used in this study, provided by Wolf (1983)[6], are based on a rotation order of omega, phi, kappa. This derivation is based on a counter-clockwise rotation being positive when looking down the positive end of a coordinate axis, and the rotation angles define rotation of the object coordinate axes to parallelism with the photo coordinate system for which approximations are desired. Table 1 illustrates that the angular unknowns of the center row of exposure stations are fairly simple to generate since only one rotation, in this case phi, is required.

The complication in estimation of exposure station angular unknowns results when more than one angular approximation is non-zero. This is illustrated in table 1, as the upper and lower tier of the exposure stations' angular unknowns are not simply the phi of the same photo in the middle tier with an omega of 15 degrees (plus or minus). This is because the phi angle is based on a coordinate system already rotated about its initial X axis by "omega" degrees. From table 1 it can be seen

Table 1. Camera exposure station angular unknowns (*nearest degree*).

Photo Number	Middle Circle			Bottom Circle			Top Circle		
	Omega	Phl	Kappa	Omega	Phl	Kappa	Omega	Phl	Kappa
1	0	+1	0	−13	+1	0	+13	+1	0
2	0	+31	0	−16	+30	+8	+16	+30	−8
3	0	+61	0	−27	+59	+23	+27	+59	−24
4	−4	+91	+4	−95	+76	+95	+95	+76	−95
5	0	+121	0	−155	+56	+159	+155	+56	−159
6	0	+151	0	−165	+28	+173	+165	+28	−173
7	0	+181	0	+13	+181	0	−14	+181	0
8	0	−149	0	−164	−30	+188	+164	−30	−188
9	0	−119	0	−154	−58	+203	+154	−58	−203
10	−2	−89	−2	−85	−76	−84	+84	−77	+84
11	0	−59	0	−25	−56	−21	+25	−56	+21
12	0	−29	0	−15	−28	−7	+15	−28	+7

that the top circle and bottom circles' phi's are equal, with the omegas and kappas equal in magnitude, but opposite in sign.

The authors have used a simplistic, though effective, procedure in estimation of angular orientation parameters to within 20 degrees of their actual value, which is sufficient for solution of the linearized equations in most convergent photogrammetric work. In this process, a sheet of paper is treated as the object X-Y plane (positive X horizontal to the right, positive Y upwards, thus the Z axise is positive towards you). With practice, a person can effectively rotate the X, Y, Z axes in succession towards any camera orientation. This can be practiced using the approximations listed in table 1, noting that after rotation the proper camera orientation has been achieved.

(2) Control Configuration and Target Arrangement

96 targets were positioned on the vertical sides of the cylindrical object in three horizontal circles, spaced 23 cm. apart, of 32 equally spaced targets each. Nine additional points were positioned on the object by theodolite triangulation (instrument least count of 0.5 seconds), with five of these spaced between the upper and middle row of unknown targets, and the other four spaced between the lower and middle rows. The role of the number of control points, and their relative positions on the object, on the bundle adjustment solutions is a variable which will be fully analyzed in this paper.

(3) Transformation of Plate Coordinates to the Photo Coordinate System

After all targets on a photograph have been identified and measured in a monoscopic mode on the DSR-11; all comparator coordinates were corrected for systematic errors in the measuring system based on caliberation parameters from a measurement of a precise grid plate. All targets were measured twice and averaged, with a coordinate discrepancy of more than 10 microns used as a remeasurement tolerance. For the metric photographs, an affine transformation (Wolf, 1983),[6] based on fiducial mark measurement, was used to transform the comparator coordinates to the photo coordinate system. Systematic error corrections were then applied for radial lens

distortion, and for the principal point of autocollimation not being at the photocoordinate origin, based upon the camera's calibration report.

Since one of the particular interests of this investigation involved the accuracy attainable with a "quality" non-metric camera without any form of calibration information, the only systematic correction of the non-metric coordinates was for the comparator's systematic errors. The image format corners were used in defining a photocoordinate system (Hintz, 1985)[5], and no attempt was made to accurately calibrate the principal distance, the principal point location, or any systematic distortions.

3. Analysis of Results

(1) Consistent Parameters Utilized in all Presented Results

All photocoordinates were assigned standard error estimates of 3 microns for all adjustments and all control coordinates were treated as "absolutely" known. The systematic error in control coordinates, due to measurement errors in their determination by theodolite triangulation, will be shown is several ways. All standard errors are based on the actual post-adjustment results, except where "simulated" indicates the standards errors illustrated are based on the preadjustment measurement standard error estimates, and the camera network geometry.

All stanandard errors presented represent the average of the standard errors for all unknown coordinate standard errors in a particular adjustment. If an average standard error is not designated as X, Y, or Z it indicates all three coordinate errors have been cumulatively averaged for a certain adjustment.

Since the location of control points in varied directions on a cylindrical object requires a series of theodolite setups for position determination by intersection, it is obvious that the location of a large set of control points, circling the entire cylindrical object, is a time consuming process that is subject to error. The results will not only illustrate the change in precision as the number of control points is dropped from nine to the minimal configuration of two X, Y and three Z control coordinates (which will be referred to as "2" cotrol points to distinguish it from three 3-D control points), but also the difference in results when control points are reduced "sequentially" (clockwise) around the object compared to the same number of control points equally distributed around the object ("even"). This comparison is important as the sequential distribution requires less theodolite setups, and is thus less time consuming and error-prone.

(2) The Comparison of the 12, 24, and 36 Metric Photo Cases

Figures 2, 3, and 4 illustrate the average coordinate standard errors vs. number of control points ("sequential" distribution) for the 12, 24, and 36 photo cases respectively, with the 24 photo case utilizing the lower and upper circles of exposures. The first item evident from figure 2 is that the 12 photo case has very equipment errors in all three dimensions when more than four control points are utilized, while the Y coordinate is significantly more precise than the X or Z coordinates when less than four control points are utilized. Figure 2 illustrates that in the 24 photo case the opposite situation is apparent. The 36 photo case indicates the same beha-

vior as the 24 photo case. The camera network geometry is the reason for this trend, as the 24 and 36 photo case differ from the 12 photo case in that convergent camera axes exist in two dimensions instead of one.

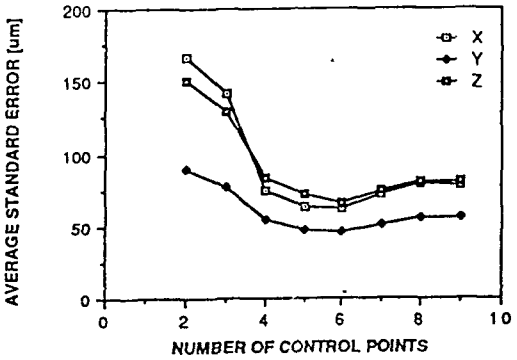

Fig. 2 Average coordinate standard error for 12 photo cate.

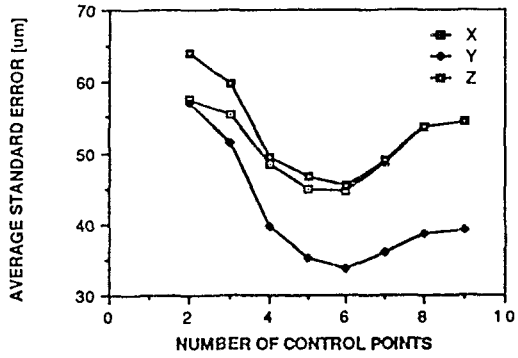

Fig. 3 Average coordinate standard error for 24 photo case.

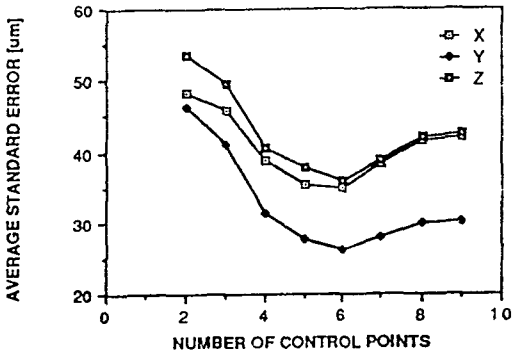

Fig. 4 Average coordinate standard error for 36 photo case.

The second noticeable trend illustrated in figures 2, 3, and 4 is that the standard errors drop much more significantly from 12 to 24 photos than between 24 and 36 photos. This is attributable to the increase in the strength of the camera network geometry, as the 12 photo solution has convergent camera axes in the X (horizontal) direction only, while the 24 photo case has convergence in both the horizontal and vertical directions.

The final important fact illustrated in figures 2, 3, and 4 is that the precision increase is dramatic as the number of control points is incremented from three to four. An increase from four to six control points resulted in a very insignificant increase in precision. If more than six control points were used,

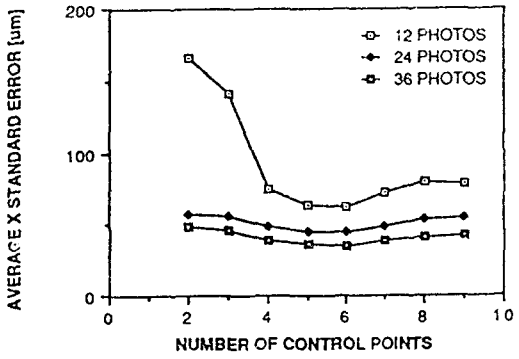

Fig. 5 Comparison of average X coordinate standard error for 12, 24, and 36 photos.

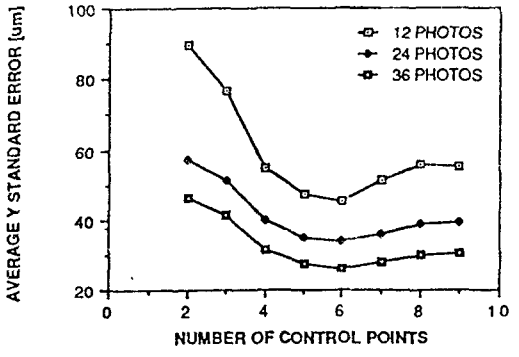

Fig. 6 Comparison of average Y coordinate standard error for 12, 24 and 36 photos.

the systematic error in their positions actually made the post-adjustment standard errors grow. This indicates that theodolite triangulation of more than four control points appears impractical.

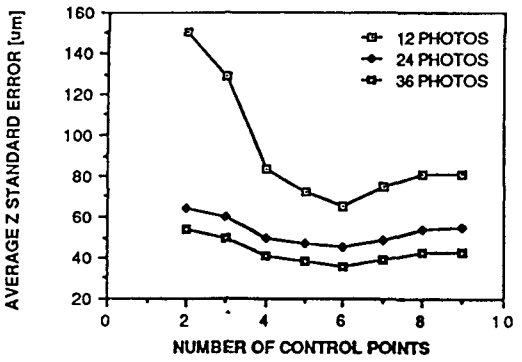

Fig. 7 Comparison of average Z coordinate standard error for 12, 24 and 36 photos.

Figures 5, 6, and 7 relate the average standard error of X, Y, and Z coordinates, respectively, for the 12, 24, and 36 photo situations. These figures further illustrate the trends presented in figures 1, 2, and 3. The dramatic increase in precision from the 12 to 24 photo case, and the insignificant increase in precision from 24 to 36 photos, is perhaps better illustrated. The increase in precision from 3 to 4 control points, and the lack of increase in precision resulting from additional control points after four, is also better illustrated.

(3) Illustration of Control Point Coordinate Error Contribution and Location of Control Points on the Solution

Figure 8 illustrates two important comparisons using the cumulative average of all three coordinate standard errors. While actual error represents the post-adjustment standard error estimates, the simulated average standard error is determined from the object coordinate errors based on a variance-covariance matrix which is solely derived from the pre-adjustment measurement error estimates, i. e., three microns for all photocoordinates. Figure 8 indicates that the three micron error estimate is probably slightly smaller than the actual error in the photocoordinates, since the actual error is always larger than its simulated equivalent.

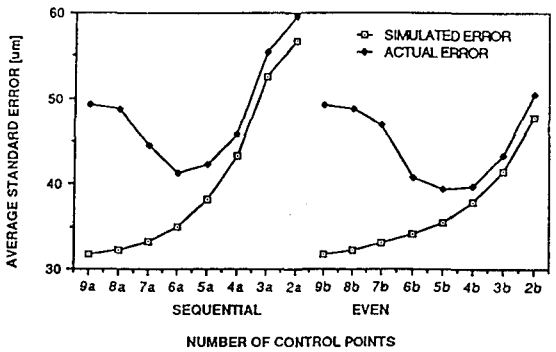

Fig. 8 Effect of control point location on 24 photo solution.

It is evident that the error in the control points is a significant contributor to the photocoordinate residuals for an adjustment, as the difference between the simulated and actual errors decreases as the number of control points decrease. Actual error becomes significantly closer to simulated error in the decrease from seven to six control points. The decrease from four to minimal control configuration shows little change in the difference

between actual and simulated error. This is interesting since the four control point situation also had significance in figures 2-7, which illustrated that actual error decreased significantly as the number of control points was increased from three to four. Figure 8 also illustrates the difference between sequential control points, where a small number of control points indicates a significant surface of the cylinder contains no control points, compared to an even distribution of control points. When the number of control points is larger than four, the two control configurations are essentially equivalent, since the gaps between control points do not differ appreciably in the two approaches. Four, or fewer, control points, if distributed evenly, contribute to a significantly more precise solution than four (or less) control points in close proximity.

Figure 9 is a final complete comparison of both actual and simulated error for the 12, 24, and 36 photo situations. It provides a complete look at all of the discussed issues.

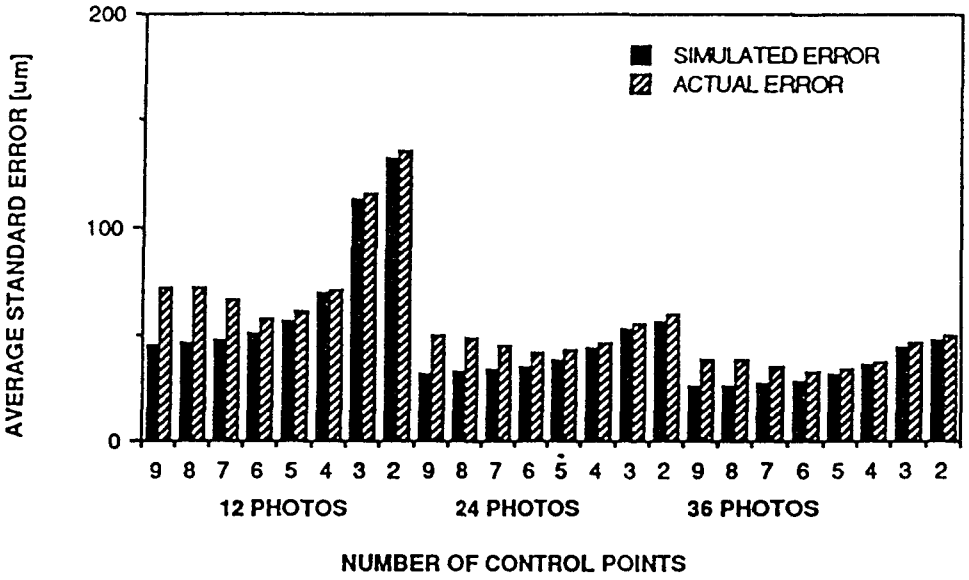

Fig. 9 Comparison of affect of control points on averaged coordinate standard error for 12, 24, and 36 photo cases.

(4) Comparisons of Solutions for Metric vs. Non-Metric Results

The 70mm. format camera was selected, over a conventional 35mm. camera, as the "test" non-metric camera as it was felt a person desiring to use a nonmetric camera for photogrammetric analysis would desire the larger image format. Any image format larger than 70mm. would definitely be an "unusual" non-metric image format. The shorter principal distance, 80.00mm vs. 105.04mm. for the P-31 camera, enabled very similar photo overlaps when exposed from approximately the same exposure stations, which were approximately 1.8 meters from the test cylinder. The same principal distance for the non-metric camera would have resulted in an increase in photographic scale, which logically increases precision. Unfortunately, it would also have decreased the photographic cover-

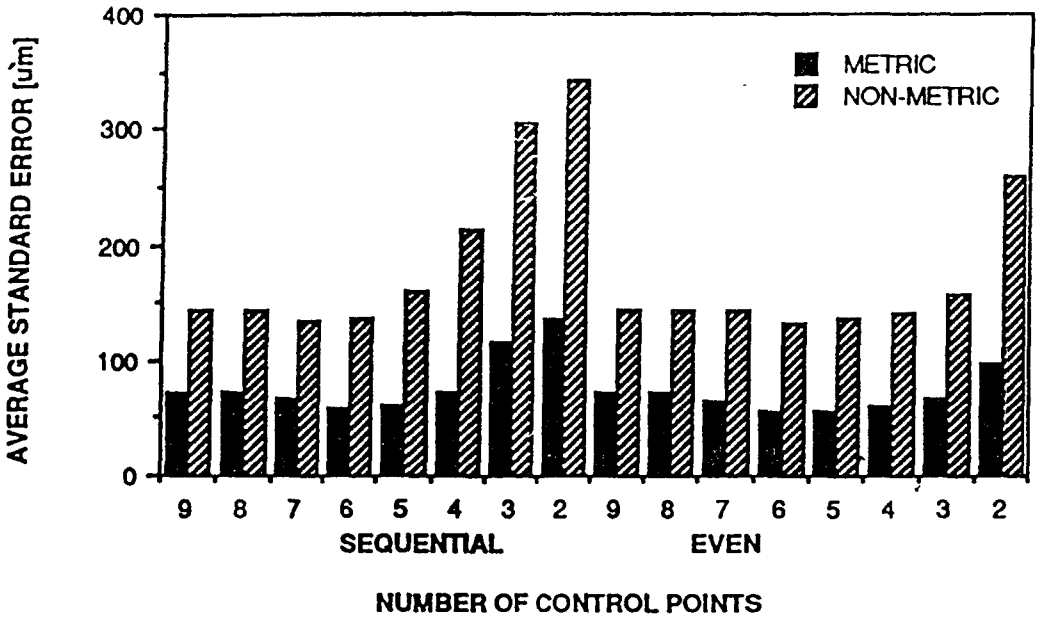

Fig. 10 Comparison of affect of control point location on averaged standard errors for 12 photo metric and non-metric solutions.

age, resulting in more photos or a longer object distance. To eliminate all of these variables, the non-metric photographs were taken from the same exposure stations as were used for the middle circle of 12 metric photos.

Figure 10 compares the average standard error for the metric 12 photo adjustments with the equivalent non-metric adjustments. Both sequential "elimination" of control points and an even distribution of control points is illustrated. While the standard errors are larger for the non-metric cases, it should be noted the object coordinate standard errors are illustrated in microns, so even the minimal control configuration produces average standard errors of less than 350 microns for the non-metric 12 photo adjustment. It is felt the accuracy achieved by the non-metric adjustments should be of a high enough quality for many close-range measurement problems.

Figure 11 provides an illustration of the

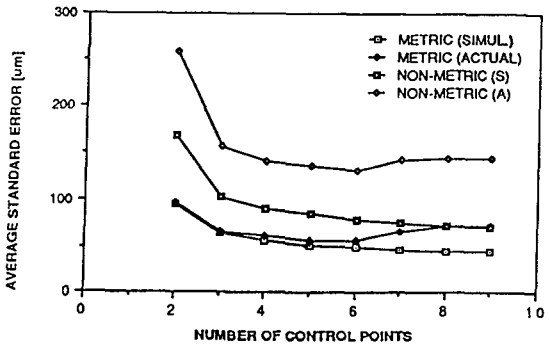

Fig. 11 Comparison of simulated and actual metric vs. non-metric 12 photo solutions.

effect of the errors induced by not calibrating the non-metric camera. Since the coordinates of all photos were measured with the same procedures using the same measuring device (the analytical stereoplotter in a monoscopic mode), the larger differences between the simulated and actual errors in the non-metric situation is partially due to the systematic errors which can be corrected by camera

calibration. Larger random errors, due to items such as film non-flatness, also contribute to the larger difference between simulated and actual error in the non-metric cases.

The larger errors due to non-calibration and a non-metric camera obviously will create errors in the adjusted object coordinates-the question is "how large?" This can be illustrated by a direct comparison of adjustment coordinates (metric vs. non-metric) for the same control configuration.

Figure 12, 13, and 14 illustrate the distri-

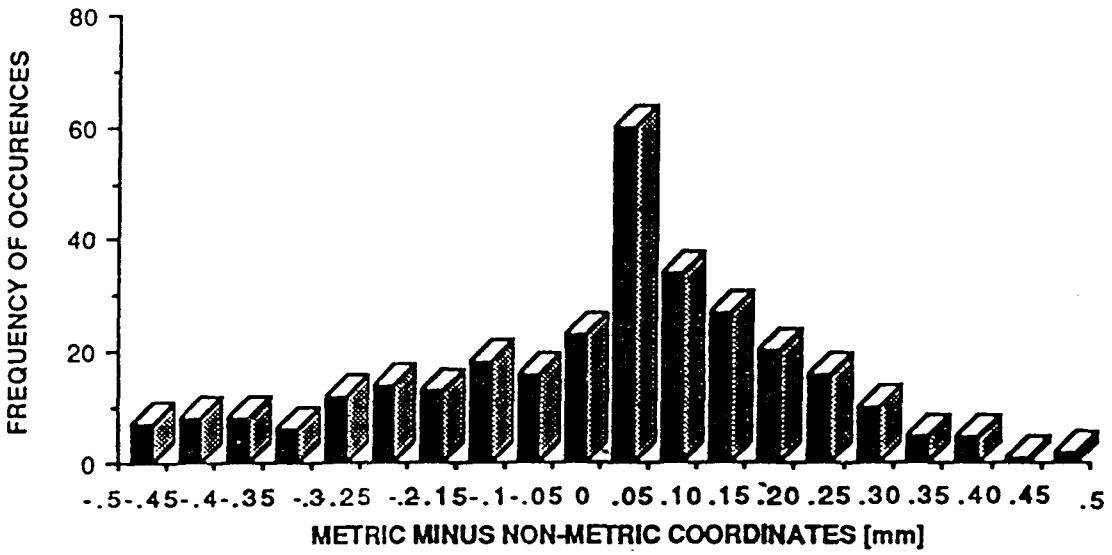

Eig. 12 Coordinate differences (metric minus non-metric) of 12 photo solutions with 9 points.

bution for metric minus non-metric adjusted object coordinates for the same points for nine control points, six control points, and minimal object control configuration (2X, Y; 3Z) adjustments respectively. Notice as the number of control points decrease, not only do larger coordinate differences exist, as should be expected, but the appearance of the frequency distribution also begins to look less like a normall (bell shaped) distribution. The larger control point configuration essentially constrains the solution to conform more to the defined object coordinate system, and thus the object space coordinates are not as "free" to adjust based on the systematic errors introduced into the adjustment by a lack of calibration.

To enable the same X axis to be used in figures 12, 13 and 14 a″ coordinate differences whose absolute values were larger than 0.5 mm. were not shown. 10 coordinate differences fell into this category for the nine control point case, 15 coordinate differences were in this group for the six control point situation, and in the minimum control configuration case 123 coordinate differences had an absolute value of more than 0.5mm. This illustrates the systematic error contributions to the non-metric solution.

Do figures 12, 13, and 14 illustrate larger coordinate differences than should be expected? To look at this, one should refer to the standard errors illustrated in figure 11 that correspond to figures 12, 13, and 14. For nine

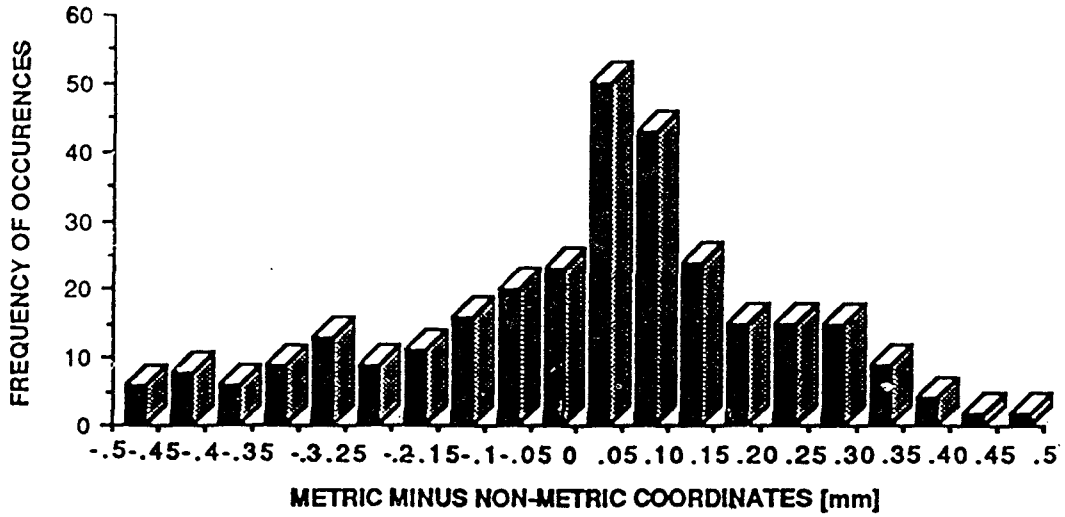

Fig. 13 **Coordinate differences (metric mnus non-metric) of 12 photo solutions with 6 control points.**

control points, metric and non-metric average standard errors are 80 and 150 microns respectively. From figure 12, 56% of the differences are less than 80 microns, and 67% of the differences are less than the 150 micron average standard error. Notice the 67% compares very closely to the amount of data within one "sigma" of actual for a normal distribution curve.

As a comparison, the minimal control configuration case results in average coordinate standard errors of 100 microns and 250 microns for the metric and non-metric 12 photo adjustments respectively. Referring to figure

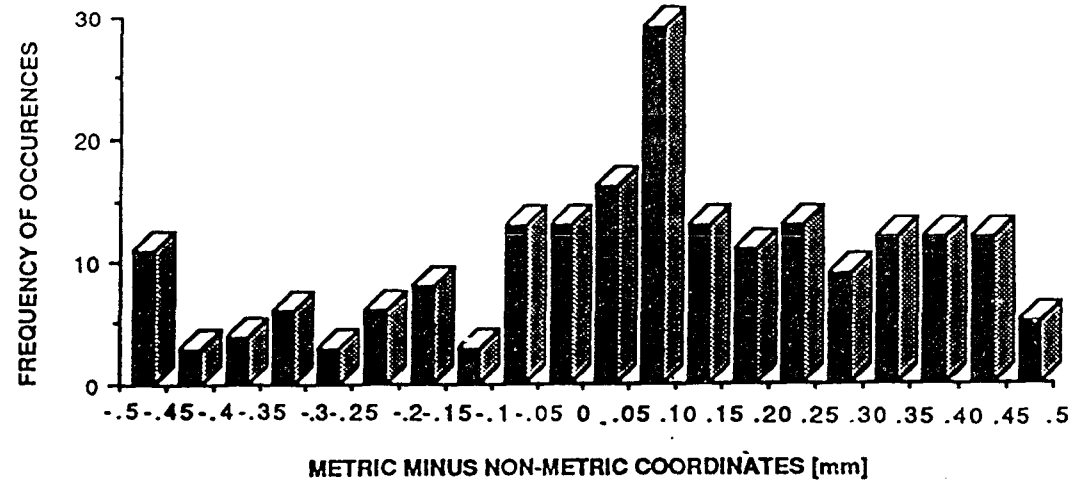

Fig. 14 Coordinate differences (metric minus non-metric) of 12 photo solutions with minimum control configuration (2 X,Y; 3Z).

14, 24% of the differences are less than 100 microns, and 43% are less than 250 microns. The drop in percent of differences within one standard error is directly attributable to the contribution of errors due to a lack of calibration in the nonmetric case. These results illustrate some of the thought which must go into the decision as to whether an uncalibrated non-metric camera will provide suitable results.

4. CONCLUTIONS

A practical of the use of convergent metric and non-metric photogrammetry in the determination of three-dimensional positions on a circular or cylindrical object has been provided.

1. It has been shown that more than 4 control points in the solution does not appreciably enchance the precisions achievable in a undle adjustment procedure.
2. The simulated average standard errors drop some 41% and 52%, the actual average standard errors drop some 40. 8% and 52. 5% as changing the number of photos from 12 to 24 and 36. The standard errors drop much more significantly from 12 to 24 photos than from 24 to 36 photos. This is attributable to the increase in the strength of the camera network geometry.
3. While the use of non-metric photography has been shown to provide accuracy which will solve many measurement problems, it has also been illustrated that the systematic errors in a solution from a noncalibrated camera can substantially perturb the solution for the object coordinates beyond their adjustment standard error estimates.

Acknowledgements

The authors wish to thank Korean Science Foundation that sponsored for this study, Mr. Mike Z. Zhao, a graduate student in Surveying Engineering at the University of Maine, for his help in preparation of all illustrations in this paper, and graduate students in Surveying & Photogrammetry at the Chung-Nam National University for their help in experiment of this study.

REFERENCES

1. Fraser, Clive S. 1986, "Photogrammetric Measurement of Thermal Deformation of Large Scale Compressor," PE & RS, pp. 1569~1575.
2. Brown, D. C., 1980, "Application of Close-Range Photogrammetry to Measurement of Structures in Orbit," Vol. 1, Geodetic Services Incorporated Technical Report No. 80-012, Melbourne, Florida, p. 131.
3. Haim, B. Papo, 1985, "Deformation Analysis by Close-Range Photogrammetry," PE & RS, pp. 1561~1597.
4. Brandenberger, A. J. & S. K. Ghosh, 1983, "Deformation Measurements of Power Dams with Aerial Photogrammetry," PE & RS, Vol. 49, No. 11, pp. 1561~1567.
5. Hintz, R. J., 1985, "Direct Input of Comparator Coordinates into an Analytical Bundle Adjustment," *Poceedings of the American Society for Photogrammetry and Remote Sensing Fall Technical Meeting*, Indianapolis, Indiana, pp. 573~581.
6. Wolf, P. R., 1983, *Eliments of Photogrammetry*, McGraw-Hill, Inc., New York, New York, p. 628.
7. Fryer, John G. & Duane C. Brown, 1986, "Lens Distortion for Close-Range Photogrammetry," PE & RE, Vol. 11, No. 1, pp. 51~58.
8. Davidson, J. L., 1985, "Stereo Photogrammetry in Geotechnical Engineering Research," PE & RS, Vol. 51, No. 10, pp. 1589~1596.
9. HIntz, Reymond J., Ioant, Thomas M. D & Richard K. Merchant, 1985, "Delineation of Graniofacial Abnomalities of the Fadal Alcohol Syndrom by Close-Range Photogrammety," PE & RS.
10. Hintz, R. J & J. M, Kang, 1985, "An Analysis of the Effect of Varying Camera Positions on the Accuracies Attainable by Non-Convergent Close-Range Photogrammetry," ASP-ACSM Convention, Vol. 1, pp. 55~61.